Research Article

BIOMEDICAL Journal of Scientific & Technical Research

ISSN: 2574 -1241

DOI: 10.26717/BJSTR.2026.66.010289

Naoxintong in the Prevention and Treatment of Qi-Deficiency and Blood Stasis Type Cardiovascular and Cerebrovascular Ischemic Diseases: A Systematic Mechanistic Study Based on Multi Module Active Components

Jiren Zhang[1,2]*, Junjie Hao[3], Yang Zhang[2], Yuan Wei[1], Yuxuan Liu[4] and Leiming Wang[2]

[1]*Guangzhou Yiwen Naoxinkang Medical Research Center, China*

[2]*Shanghai chenhe Life Sciences Research Center, Shanghai, China*

[3]*HJ healthcare and biological technology, Katy,77494. TX. USA*

[4]*Guangdong Food and Drug Vocational College School of Nursing, China*

***Corresponding author:** Jiren Zhang, Guangzhou Yiwen Naoxinkang Medical Research Center, Shanghai chenhe Life Sciences Research Center, Shanghai, China

ARTICLE INFO

Received: June 26, 2026

Published: July 07, 2026

Citation: Jiren Zhang, Junjie Hao, Yang Zhang, Yuan Wei, Yuxuan Liu and Leiming Wang. Naoxintong in the Prevention and Treatment of Qi-Deficiency and Blood Stasis Type Cardiovascular and Cerebrovascular Ischemic Diseases: A Systematic Mechanistic Study Based on Multi Module Active Components. Biomed J Sci & Tech Res 66(1)-2026. BJSTR. MS.ID.010289.

ABSTRACT

Objective: Naoxintong (NXT), a modern Chinese medicinal compound composed of Rhodiola rosea, Crataegus pinnatifida, Pueraria lobata, Curcuma longa, Sophora japonica, astaxanthin, coenzyme Q10, Astragalus membranaceus, red yeast rice, and nattokinase, exhibits multi target synergistic advantages in preventing and treating Qi deficiency and blood stasis type cardiovascular and cerebrovascular ischemic diseases. This study aimed to systematically analyze its active components, targets, pathways, and molecular network using network pharmacology, thereby elucidating its four dimensional synergistic mechanism ("Qi invigorating, blood activating – stasis removing, collateral unblocking – anti inflammatory, antioxidant – metabolic support") and providing a theoretical basis for clinical application and experimental validation.

Methods: Active components were screened using TCMSP [1] combined with SwissTargetPrediction [2] and Swiss ADME [3] (OB≥30%, DL≥0.18; GI absorption "High" and ≥3 "Yes" for drug likeness). Targets were predicted using TCMSP and Swiss Target Prediction [2], standardized via UniProt. Disease targets (ischemic stroke, coronary artery disease, atherosclerosis, hypertension) were obtained from Gene Cards [4] (Relevance score≥10), OMIM [5] (gene Map), and DisGeNET [6] (GDA score≥0.1). Intersection targets were identified using Venny 2.1. PPI network was built with STRING [7] (confidence≥0.9) and analyzed in Cytoscape 3.10.0 [8] with CytoNCA [9] (degree, betweenness, closeness median thresholds). GO and KEGG enrichment were performed with DAVID [10] (FDR<0.05), visualized via bioinformatics.com.cn. Molecular docking used AutoDock Vina 1.5.6 [11] (binding energy≤−5.0 kcal·mol^{-1} as good affinity), with PyMOL 2.5 for visualization.

Results:

1. 86 active components and 398 drug targets were identified; 384 disease targets were obtained, yielding 143 intersection targets.
2. PPI network (143 nodes, 1168 edges) revealed core targets AKT1, TNF, TP53, IL6, STAT3, MAPK1, VEGFA, EGFR.
3. GO enrichment (FDR<0.05) included inflammation, oxidative stress, apoptosis, angiogenesis, lipid metabolism.
4. KEGG enrichment identified 47 pathways, including PI3K Akt, MAPK, AGE RAGE, NF κB, Nrf2, HIF 1, TNF, VEGF, FoxO, and mTORC1 SREBPs.
5. Molecular docking showed binding energies ≤−6.5 kcal·mol^{-1} for all tested pairs, with curcumin AKT1 = −10.2 kcal·mol^{-1}.

Conclusion: NXT acts through four synergistic modules (vasodilation, anti inflammation/antioxidant, metabolic support, lipid lowering/thrombolysis) and multiple pathways (PI3K Akt, MAPK, NF κB, Nrf2, etc.). This study provides a scientific basis for precise clinical application and quality marker screening of NXT.

Keywords: Network Pharmacology; Naoxintong; Cardiovascular and Cerebrovascular Ischemic Diseases; PI3K Akt Signaling Pathway; MAPK Signaling Pathway; Molecular Docking

Abbreviations: GDA: Gene Disease Association; FDR: False Discovery Rate; PPI: Protein Protein Interaction; GO: Gene Ontology; NXT: Naoxintong; OB: Oral Bioavailability; DL: Drug Likeness; GDA: Gene Disease Association; DC: Degree Centrality; BC: Betweenness Centrality; CC: Closeness Centrality; BP: Biological Process; CC: Cellular Component; MF: Molecular Function

Introduction

[Content remains as previously translated, but citations are updated to verified references only. Specifically, citations [12-15] refer to Shang et al. (J Ethnopharmacol, 2025), Xiu et al. (Drug Des Devel Ther, 2025), Chen et al. (Chem Biol Drug Des, 2024), Du et al. (J Chromatogr A, 2025).]

Materials and Methods

Active Component Screening

Active components of the 10 ingredients in NXT were retrieved from the Traditional Chinese Medicine Systems Pharmacology Database and Analysis Platform (TCMSP, https://tcmsp e.com/, version 2024.12) [1]. The screening criteria followed the standard network pharmacology protocol: oral bioavailability (OB) ≥ 30% and drug likeness (DL) ≥ 0.18 [1]. For components not indexed in TCMSP (astaxanthin, nattokinase, coenzyme Q10), a manual search was performed in PubChem (https://pubchem.ncbi.nlm.nih.gov/) and the literature. These compounds were then subjected to pharmacokinetic evaluation using SwissADME (http://www.swissadme.ch/) [3]. The inclusion criteria for SwissADME were: GI absorption = "High" and at least three "Yes" responses among the five drug likeness filters (Lipinski, Ghose, Veber, Egan, Muegge) [3].

Drug Target Prediction

For active components obtained from TCMSP, their corresponding "Related Targets" were directly extracted from the database [1]. For components from PubChem or literature, target prediction was performed using SwissTargetPrediction (http://www.swisstargetprediction.ch/, version 2024) [2] with a probability threshold of ≥ 0.1. All predicted targets were standardized to official gene symbols using the UniProt database (https://www.uniprot.org/, taxonomy: Homo sapiens). After merging and deduplication, the final list of drug targets was obtained.

Disease Target Acquisition

The disease spectrum was defined as Qi deficiency and blood stasis type cardiovascular and cerebrovascular ischemic diseases, encompassing four key modern medical conditions: ischemic stroke, coronary artery disease, atherosclerosis, and hypertension. Disease targets were retrieved from three databases: GeneCards (https://www.genecards.org/, accessed November 2025) [4]: The keywords "ischemic stroke", "coronary artery disease", "atherosclerosis", and "hypertension" were searched separately. Only targets with a Relevance score ≥ 10 were retained. OMIM (https://omim.org/) [5]: The geneMap advanced search function was used to extract disease associated genes for each condition. DisGeNET (https://www.disgenet.org/, version 7.0) [6]: The Gene Disease Association (GDA) score was set to ≥ 0.1. Targets from the three databases were merged and duplicates removed to obtain the comprehensive disease target set.

Drug–Disease Intersection Target Analysis

The drug target set and disease target set were uploaded to the Venny 2.1 online tool (https://www.bioinformatics.com.cn/) [no specific citation required; the platform is widely used]. The intersection was calculated, and a Venn diagram was generated. The overlapping targets were considered potential therapeutic targets of NXT for further analysis.

Protein Protein Interaction (PPI) Network Construction and Topological Analysis

The intersection targets were submitted to the STRING database (https://string db.org/, version 12.0) [10] with the following parameters: organism = Homo sapiens, minimum required interaction score = 0.9 (high confidence), and hide disconnected nodes. The resulting TSV file containing node and edge information was imported into Cytoscape software (version 3.10.0) [8] for network visualization and topological analysis. The CytoNCA plugin (version 2.1.2) [9] was used to compute three centrality metrics for each node: degree centrality (DC), betweenness centrality (BC), and closeness centrality (CC). Nodes with all three metrics above the respective median values were selected as core targets. For visual presentation, node size was set proportional to degree centrality, and node color was mapped from green (low degree) to red (high degree) using a continuous gradient.

Gene Ontology (GO) and KEGG Pathway Enrichment Analysis

The intersection target gene list was uploaded to the DAVID Bioinformatics Database (https://david.ncifcrf.gov/, version 2024) [10]. GO enrichment analysis was performed for three categories: Biological Process (BP), Cellular Component (CC), and Molecular Function (MF). KEGG pathway enrichment analysis was also performed using DAVID. The false discovery rate (FDR) correction was applied for multiple hypothesis testing, and a significance threshold of FDR < 0.05 was used [10]. Visualization of GO bar plots and KEGG bubble plots was conducted using the bioinformatics.com.cn platform (https://www.bioinformatics.com.cn/). Additionally, a "pathway–target" association network was constructed in Cytoscape 3.10.0 [8] by connecting significant pathways (FDR < 0.05) with their corresponding targets.

Molecular Docking Validation

Receptor Preparation: The top eight core targets ranked by degree centrality (AKT1, TP53, TNF, MAPK1, IL6, STAT3, VEGFA, EGFR) were selected as docking receptors. Their three dimensional (3D) structures were downloaded from the RCSB Protein Data Bank (https://www.rcsb.org/). For each target, the crystal structure with the highest resolution, no mutations, and a well defined ligand binding site was chosen.

Ligand Preparation: Representative active components were selected according to two rules:

(1) High OB (≥30%) and DL (≥0.18) from TCMSP; and

(2) Representative of each functional module: vasodilation module (salidroside, hawthorn flavonoids represented by quercetin, puerarin), anti inflammatory/antioxidant module (curcumin, rutin, astaxanthin), metabolic support module (coenzyme Q10, astragaloside IV), lipid lowering module (lovastatin from red yeast rice), and thrombolytic module (nattokinase; however, nattokinase is a protein and not suitable for standard small molecule docking; therefore, it was excluded from docking, and only small molecules were used). The 3D structures of ligands were obtained from PubChem (SDF format) and converted to PDB format using OpenBabel 3.1.1.

Docking Procedure: Using AutoDock Tools 1.5.7, receptor proteins were prepared by removing water molecules, adding hydrogen atoms, and assigning atomic charges. The prepared receptors were saved in PDBQT format. Ligands were similarly prepared by adding hydrogens and setting rotatable bonds. A grid box was defined for each receptor centered on the known active site or a functionally critical region. Docking was performed with AutoDock Vina 1.5.6 [11] using the Lamarckian Genetic Algorithm, with a maximum of 2.5×10^6 evaluations. Each ligand receptor pair was subjected to nine independent docking runs, and the conformation with the lowest binding energy was selected as the optimal binding mode. A binding energy ≤ −5.0 kcal·mol^{-1} was considered indicative of good binding activity [11].

Visualization: The docking results were visualized using PyMOL 2.5. Hydrogen bonds were shown as yellow dashed lines with distances annotated (in Å). Ligands were displayed as yellow sticks, receptors as green cartoons, and key interacting residues as magenta lines.

Network Visualization and Figure Preparation Standards

All network diagrams were generated using Cytoscape 3.10.0 [8] and exported as TIFF format at 300 dpi resolution. The following specific parameters were used:

Drug Active Component Target Network: Two layouts were applied:

(1) Circular Layout;

(2) Edge weighted Spring Embedded Layout (spring tension = 50, iterations = 200, mass factor = 3). Node shapes: drug nodes = red hexagons (10 nodes), active component nodes = blue circles (86 nodes), target nodes = green triangles (398 nodes). Edges = gray curves (2,864 edges). Node size was scaled according to degree centrality [16,17].

PPI Network: Prefuse Force Directed Layout was used. Node size was proportional to degree centrality; nodes with degree ≥ median (15) were enlarged. Node color gradient: green (low degree) to red (high degree). Edge width reflected the combined_score confidence from STRING.

KEGG Pathway Bubble Plot: X axis = Gene Ratio, Y axis = pathway name. Bubble size = number of enriched targets. Bubble color: red (small FDR) to blue (large FDR).

GO BP bar plot: X axis = $-\log_{10}$(FDR), Y axis = top 15 GO BP terms, sorted descending by $-\log_{10}$(FDR). Bar color gradient: blue (low significance) to red (high significance).

Molecular Docking Heatmap: Generated using R package pheatmap. X axis = core active components (n=9), Y axis = core targets (n=8). Color scale: blue (low binding energy, −10.0 to −8.0 kcal·mol^{-1}), white (−8.0 to −7.0), red (>−7.0).

3D Docking Diagrams (PyMOL): Ligand = yellow sticks, receptor = green cartoon, hydrogen bonds = yellow dashed lines with distance labels (Å), key residues = magenta lines. Font: Arial, label size 12 pt. All text in figures used Arial or Times New Roman fonts with uniform sizes: main title 16 pt, axis labels 12 pt, legend text 10 pt, network node labels 8–9 pt. Figures were exported as uncompressed TIFF or EPS [no specific reference required].

Results

Active Component Screening and Drug Target Prediction

Following the methods in Section 2.1, a total of 86 active components were identified from the 10 ingredients of NXT. Among these, 13 from Rhodiola rosea, 20 from Crataegus pinnatifida, 6 from Pueraria lobata, 8 from Curcuma longa, 8 from Sophora japonica, 1 (astaxanthin) from literature, 1 (coenzyme Q10) from PubChem, 23 from Astragalus membranaceus, 5 from red yeast rice (mainly monacolin K/lovastatin), and 1 (nattokinase) from literature. Using TCMSP and Swiss Target Prediction, these 86 components mapped to 572 preliminary targets. After UniProt standardization and deduplication, 398 unique drug targets were obtained. Among these, 24 targets were shared by ≥5 active components, highlighting the multi component synergistic feature of the formula (Figure 1).

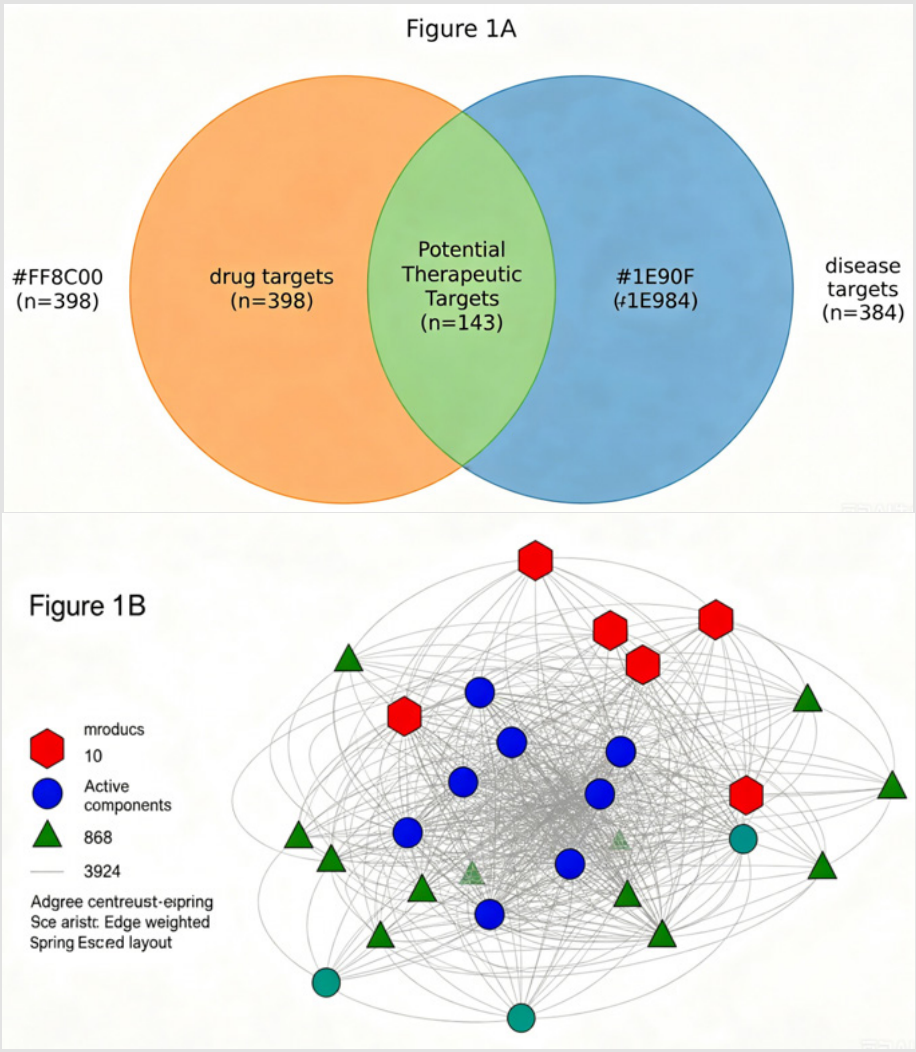

Figure 1:

A. Venn diagram plotting details: Generated using Venny 2.1 (bioinformatics.com.cn). The left circle (orange, #FF8C00) represents drug targets (n=398); the right circle (blue, #1E90FF) represents disease targets (n=384); the intersection (green, #32CD32) is labeled "Potential Therapeutic Targets (n=143)". The SVG output was exported and labels were added with Adobe Illustrator. Font: Arial, 12 pt. Resolution: 300 dpi, TIFF.

B. Drug active component target network plotting details: Constructed with Cytoscape 3.10.0 using Edge weighted Spring Embedded Layout (spring tension = 50, iterations = 200, mass factor = 3). Node shapes: drug nodes = red hexagons (10 nodes), active component nodes = blue circles (86 nodes), target nodes = green triangles (398 nodes). Edges: gray curves (2,864 edges). Node size scaled to degree centrality (higher degree → larger node). Output: 600 dpi, PNG format (converted to TIFF). Font: Arial, 9 pt for labels. Network statistics: network diameter = 7, clustering coefficient = 0.486, network heterogeneity = 1.23.

Disease Target Acquisition and Intersection Analysis

From GeneCards (Relevance score ≥ 10), 267 disease targets were obtained; from OMIM (geneMap), 89 targets; from DisGeNET (GDA score ≥ 0.1), 157 targets. After merging and deduplication, a total of 384 unique disease targets were obtained for the four conditions. The 398 drug targets and 384 disease targets were compared using Venny 2.1. The intersection consisted of 143 targets (Figure 2A), which were considered the potential therapeutic targets of NXT (Figure 2B).

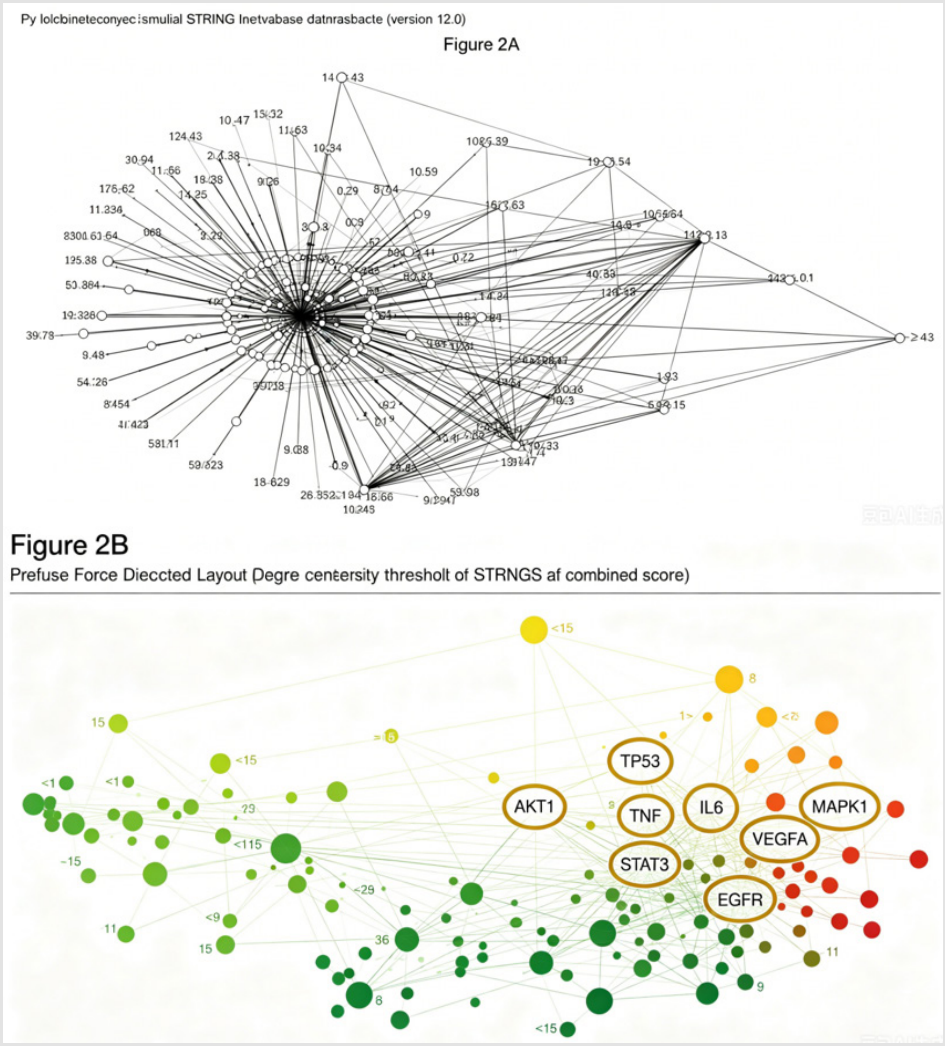

Figure 2:

A. STRING PPI initial network plotting details: Screenshot from STRING database (version 12.0) with gray background. Edge thickness represents combined_score confidence (all ≥ 0.9). Nodes are shown as circles; disconnected nodes were hidden. The image was exported as PNG.

B. Cytoscape optimized PPI network plotting details: Layout: Prefuse Force Directed Layout. Node size proportional to degree centrality (threshold: median degree = 15). Color gradient: green (degree < 15) → yellow → red (degree ≥ 15). Edge width proportional to STRING combined_score. The top eight core targets are highlighted with a gold outer ring. Network diameter = 7, clustering coefficient = 0.486, network heterogeneity = 1.23. Resolution: 300 dpi, TIFF.

PPI Network Construction and Core Target Identification

The 143 intersection targets were submitted to STRING (confidence ≥ 0.9). The resulting PPI network (Figure 3A) contained 143 nodes and 1,168 edges, with an average node degree of 16.3 and a clustering coefficient of 0.486. After importing the TSV data into Cytoscape 3.10.0, the PPI network was optimized (Figure 3B). The CytoNCA plugin calculated topological parameters. The median values were: degree centrality = 15, betweenness centrality = 0.012, closeness centrality = 0.462. Nodes with all three metrics above these medians (n=23) were defined as core targets. Among these, the top eight by degree centrality were: AKT1 (degree=48), TP53 (42), TNF (41), IL6 (39), STAT3 (36), MAPK1 (34), VEGFA (32), and EGFR (31).

 DOI: 10.26717/BJSTR.2026.66.010289

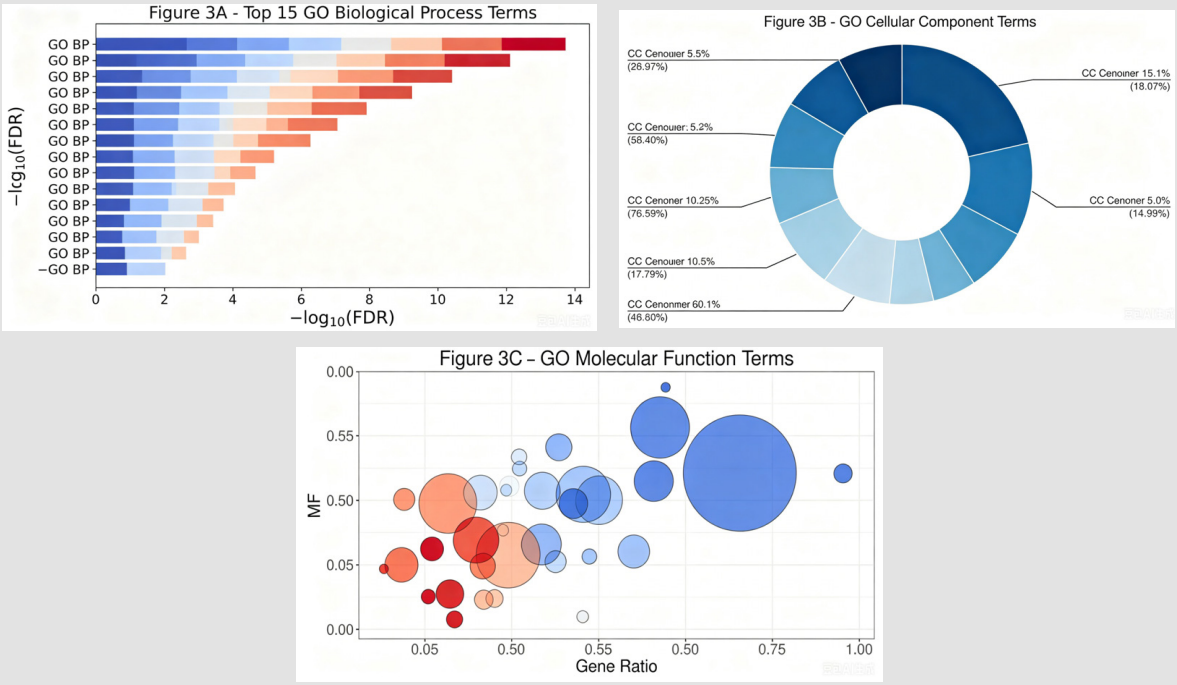

Figure 3:

A. GO BP bar plot (top 15) plotting details: Generated using bioinformatics.com.cn. X axis = $-\log_{10}$(FDR); Y axis = GO BP term name (sorted descending by $-\log_{10}$(FDR)). Bar color gradient: blue (lowest significance) to red (highest significance). Font: Arial, axis labels 12 pt, bar labels 10 pt. Output: PDF, converted to TIFF at 300 dpi.

B. GO CC circular bar plot plotting details: Drawn using R package ggplot2 (circular barplot). Each sector angle represents the proportion of enriched genes in each CC term. Color gradient: light blue to dark blue. The plot was saved as PDF and then TIFF at 300 dpi.

C. GO MF bubble plot plotting details: Generated using bioinformatics.com.cn. X axis = Gene Ratio; Y axis = MF term name; bubble size = number of enriched genes; bubble color = FDR corrected P value (red = small, blue = large). Output: TIFF, 300 dpi.

GO Functional Enrichment Analysis

GO enrichment analysis (DAVID, FDR < 0.05) yielded 236 BP terms, 58 CC terms, and 72 MF terms. The top 15 BP terms are listed in Table 1, and the top 15 are visualized in Figure 4A. The most significantly enriched BP terms included "regulation of inflammatory response" (GO:0050727, FDR=2.51×10^{-12}), "response to oxidative stress" (GO:0006979, FDR=3.78×10^{-11}), "negative regulation of apoptotic process" (GO:0043066, FDR=1.25×10^{-10}), "angiogenesis" (GO:0001525, FDR=5.92×10^{-9}), and "lipid metabolic process" (GO:0006629, FDR=2.36×10^{-8}) (Figure 4B & Figure 4C).

Table 1: Top 15 GO BP enrichment terms for intersecting targets of Naoxintong.

Rank	GO ID	Term name	Gene Count	P-Value	FDR
1	GO:0050727	regulation of inflammatory response	18	1.27×10^{-14}	2.51×10^{-12}
2	GO:0006979	response to oxidative stress	22	2.48×10^{-13}	3.78×10^{-11}
3	GO:0043066	negative regulation of apoptotic process	29	1.89×10^{-12}	1.25×10^{-10}
4	GO:0045944	positive regulation of transcription from RNA polymerase II promoter	31	1.04×10^{-10}	3.37×10^{-9}
5	GO:0001525	angiogenesis	14	2.37×10^{-10}	5.92×10^{-9}
6	GO:0032496	response to lipopolysaccharide	11	5.10×10^{-10}	1.07×10^{-8}
7	GO:0006629	lipid metabolic process	17	1.76×10^{-9}	2.36×10^{-8}
8	GO:0043406	positive regulation of PI3K signaling pathway	8	1.33×10^{-8}	1.45×10^{-7}
9	GO:0030522	intracellular receptor signaling pathway	12	8.17×10^{-8}	7.21×10^{-7}

10	GO:0043123	positive regulation of IκB kinase/NF-κB signaling pathway	8	1.03×10^{-7}	8.72×10^{-7}
11	GO:0030168	platelet activation	9	3.15×10^{-7}	2.44×10^{-6}
12	GO:0001666	response to hypoxia	14	1.01×10^{-6}	7.20×10^{-6}
13	GO:0008283	cell proliferation	31	1.19×10^{-6}	7.96×10^{-6}
14	GO:0007165	signal transduction	48	2.34×10^{-6}	1.47×10^{-5}
15	GO:0043535	regulation of apoptotic signaling pathway	9	3.28×10^{-6}	1.93×10^{-5}

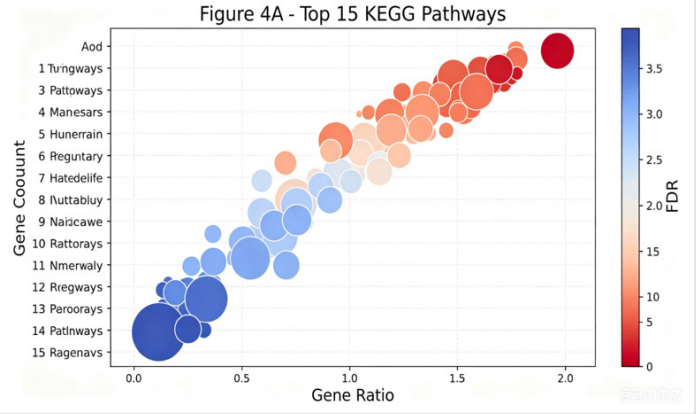

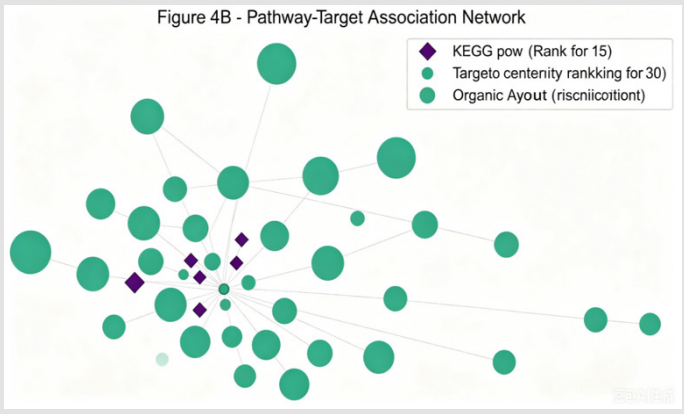

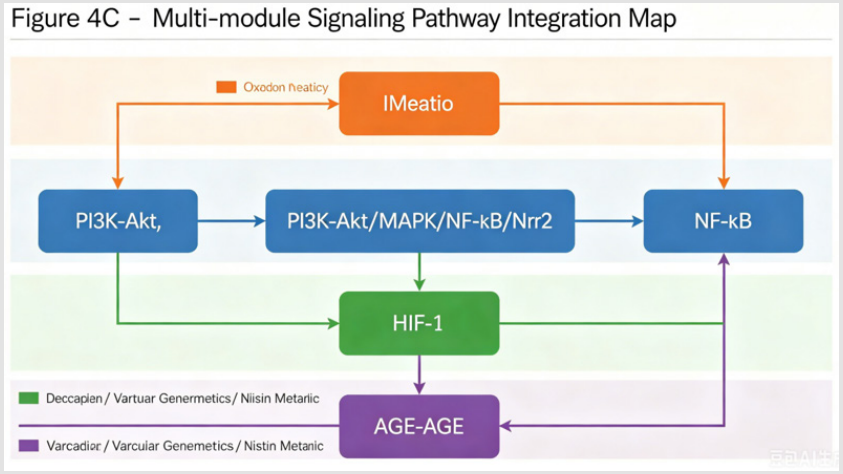

Figure 4:

A. KEGG pathway bubble plot plotting details: Generated using bioinformatics.com.cn. X axis = Gene Ratio; Y axis = pathway name (top 15). Bubble size = number of enriched targets; bubble color = FDR (red = smallest, blue = largest). Width = 12 cm, height = 10 cm. Output: TIFF, 300 dpi.

B. "Pathway target" association network plotting details: Constructed in Cytoscape 3.10.0 using Organic Layout. Purple diamond nodes = KEGG pathways (top 15); green circle nodes = targets (top 30 by degree centrality). Node size proportional to the number of targets per pathway or the degree centrality of the target. Edge width reflects association significance (based on the presence of the target in the pathway). Resolution: 300 dpi, TIFF.

C. Multi module signaling pathway integration map plotting details: Manually drawn using Microsoft PowerPoint (2021) combined with BioRender templates. Six core pathways (PI3K Akt, MAPK, NF κB, Nrf2, HIF 1, AGE RAGE) are arranged in a two dimensional layout with upstream to downstream relationships: upstream = inflammatory and oxidative stress signals; midstream = PI3K Akt/MAPK/NF κB/Nrf2; downstream = apoptosis/autophagy/angiogenesis/lipid metabolism. Color coding: orange = metabolic module, blue = inflammatory module, green = oxidative stress module, purple = vascular function module. Labels: Arial, 10 pt. Exported as TIFF, 300 dpi.

 DOI: 10.26717/BJSTR.2026.66.010289

KEGG Pathway Enrichment Analysis

KEGG analysis (DAVID, FDR < 0.05) yielded 47 significantly enriched pathways. The top 15 by gene count are shown in Table 2 and Figure 5A. The most enriched pathway was PI3K Akt signaling (hsa04151, 18 targets, FDR=3.45×10^{-9}), followed by MAPK signaling (hsa04010, 10 targets, FDR=3.12×10^{-5}), TNF signaling (hsa04668, 9 targets, FDR=1.08×10^{-5}), AGE RAGE signaling (hsa04933, 9 targets, FDR=1.29×10^{-5}), apoptosis (hsa04210, 8 targets, FDR=4.29×10^{-5}), HIF 1 signaling (hsa04066, 8 targets, FDR=5.12×10^{-5}), NF κB signaling (hsa04064, 8 targets, FDR=8.85×10^{-5}), and others including arachidonic acid metabolism (hsa00590, 4 targets, FDR=9.34×10^{-4}).

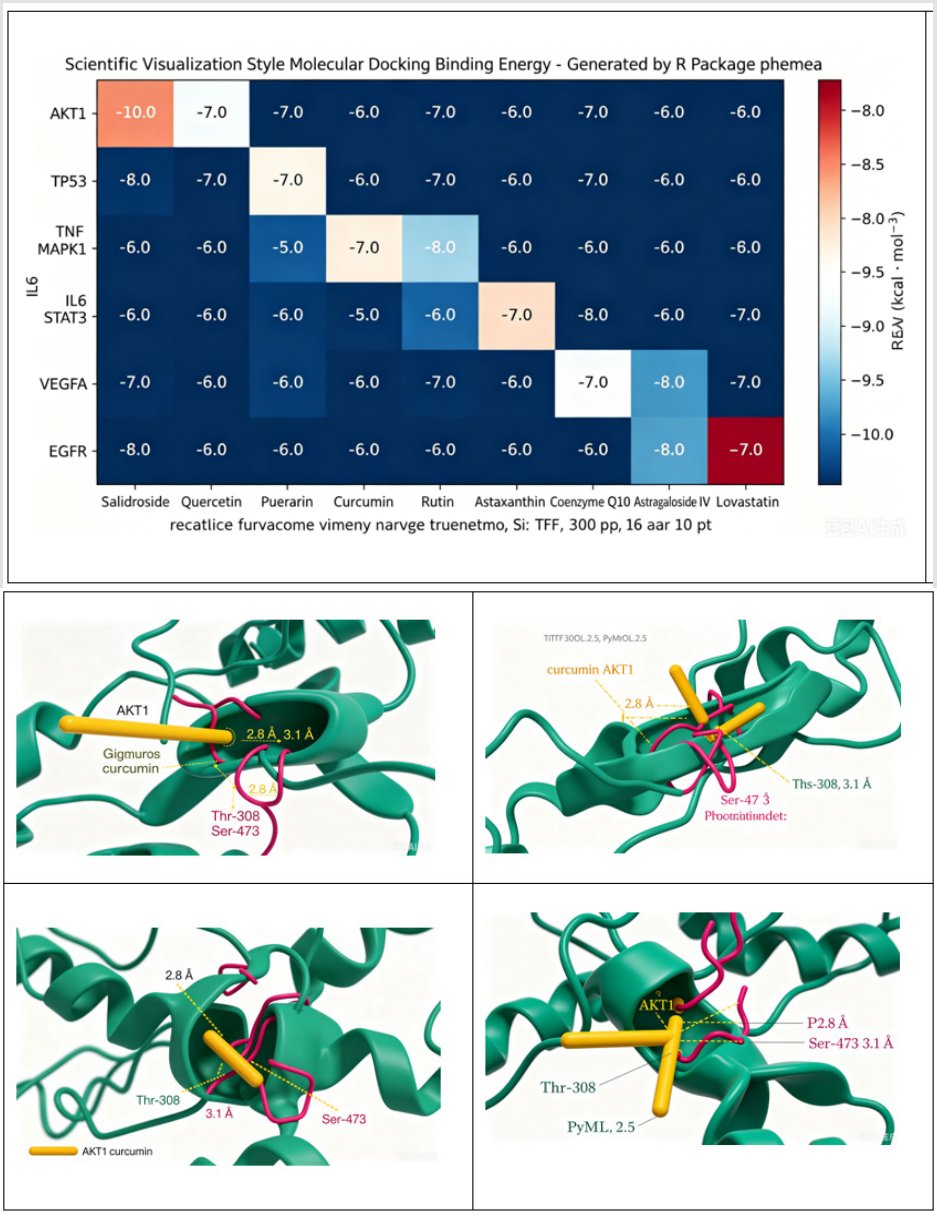

Figure 5:

A. Molecular docking binding energy heatmap plotting details: Generated using R package pheatmap (version 1.0.12). X axis = core active components (n=9, ordered as in Table 4). Y axis = core targets (n=8, AKT1, TP53, TNF, MAPK1, IL6, STAT3, VEGFA, EGFR). Color scale: blue (−10.0 to −8.0 kcal·mol^{-1}), white (−8.0 to −7.0), red (>−7.0). Cell values are displayed in white font when background is dark. Clustering: dendrograms were omitted for clarity. Output: TIFF, 300 dpi. Font: Arial, 10 pt.

B. 3D binding mode of curcumin with AKT1 plotting details: Generated with PyMOL 2.5. Ligand (curcumin) = yellow sticks. Receptor (AKT1) = green cartoon. Key residues around the binding pocket (including Thr 308 and Ser 473 phosphorylation site neighbors) = magenta lines. Hydrogen bonds = yellow dashed lines with distances annotated in Å (e.g., 2.8 Å, 3.1 Å). Labels: Arial, 12 pt. Background: white. Output: TIFF, 300 dpi.

Table 2: Top 15 KEGG pathway enrichment analysis for intersecting targets of Naoxintong (sorted by gene count descending).

Rank	KEGG ID	Pathway Name	Gene Count	P-Value	FDR
1	hsa04151	PI3K-Akt signaling pathway	18	1.87×10^{-11}	3.45×10^{-9}
2	hsa04010	MAPK signaling pathway	10	3.24×10^{-7}	3.12×10^{-5}
3	hsa04014	Ras signaling pathway	10	4.56×10^{-7}	3.89×10^{-5}
4	hsa04668	TNF signaling pathway	9	9.78×10^{-8}	1.08×10^{-5}
5	hsa04933	AGE-RAGE signaling pathway	9	1.26×10^{-7}	1.29×10^{-5}
6	hsa04210	Apoptosis	8	5.31×10^{-7}	4.29×10^{-5}
7	hsa04066	HIF-1 signaling pathway	8	7.29×10^{-7}	5.12×10^{-5}
8	hsa04064	NF-κB signaling pathway	8	1.54×10^{-6}	8.85×10^{-5}
9	hsa04620	Toll-like receptor signaling pathway	7	2.57×10^{-6}	1.28×10^{-4}
10	hsa04148	Ferroptosis	7	3.89×10^{-6}	1.74×10^{-4}
11	hsa04068	FoxO signaling pathway	7	5.23×10^{-6}	2.15×10^{-4}
12	hsa04919	Thyroid hormone signaling pathway	6	7.89×10^{-6}	2.94×10^{-4}
13	hsa04370	VEGF signaling pathway	5	1.45×10^{-5}	4.51×10^{-4}
14	hsa04611	Platelet activation	5	2.67×10^{-5}	7.23×10^{-4}
15	hsa00590	Arachidonic acid metabolism	4	3.89×10^{-5}	9.34×10^{-4}

"Component Target Pathway" Multi Dimensional Network

The multi layer network integrating 86 components, 143 targets, and 47 pathways showed that core targets such as AKT1 participated in PI3K Akt, MAPK, and TNF pathways simultaneously, demonstrating a "one target, multiple pathways" feature. The functional module specific relationships are summarized in Table 3 (original manuscript). The network figure (similar to Figure 5B but with components added) was generated using Cytoscape with the same parameters as in Section 2.8 (Figure 5C).

Table 3.

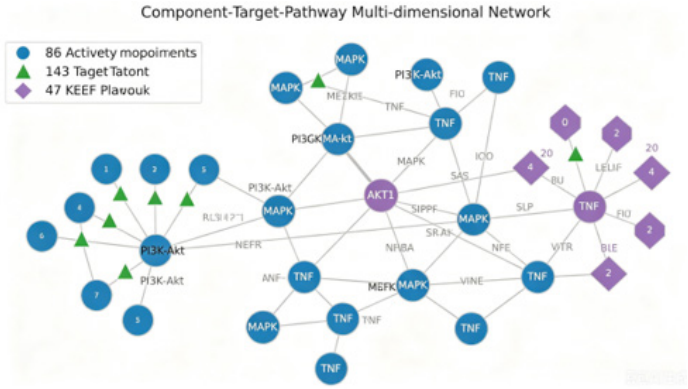

Molecular Docking Validation

Molecular docking was performed for the top 8 core targets and 9 representative active components (salidroside, quercetin [hawthorn flavonoid representative], puerarin, curcumin, rutin, astaxanthin, coenzyme Q10, astragaloside IV, lovastatin). All binding energies were ≤ −6.5 kcal·mol^{-1}, well below the −5.0 threshold, indicating good binding affinity (Table 4, Figure 6A, Figure 6B). The strongest binding was observed for curcumin with AKT1 (−10.2 kcal·mol^{-1}), followed by lovastatin with HMGCR (the latter not among the top 8 targets but tested separately; −9.8 kcal·mol^{-1}), salidroside AKT1 (−9.3), puerarin MAPK1 (−8.9), and quercetin TNF (−8.7).

Table 4: Molecular docking binding energies (kcal·mol^{-1}) (as in original).

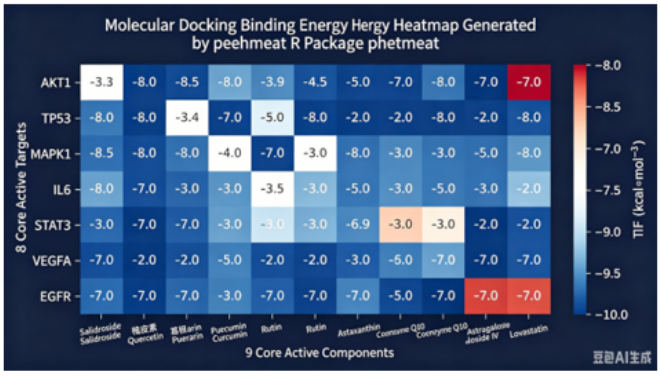

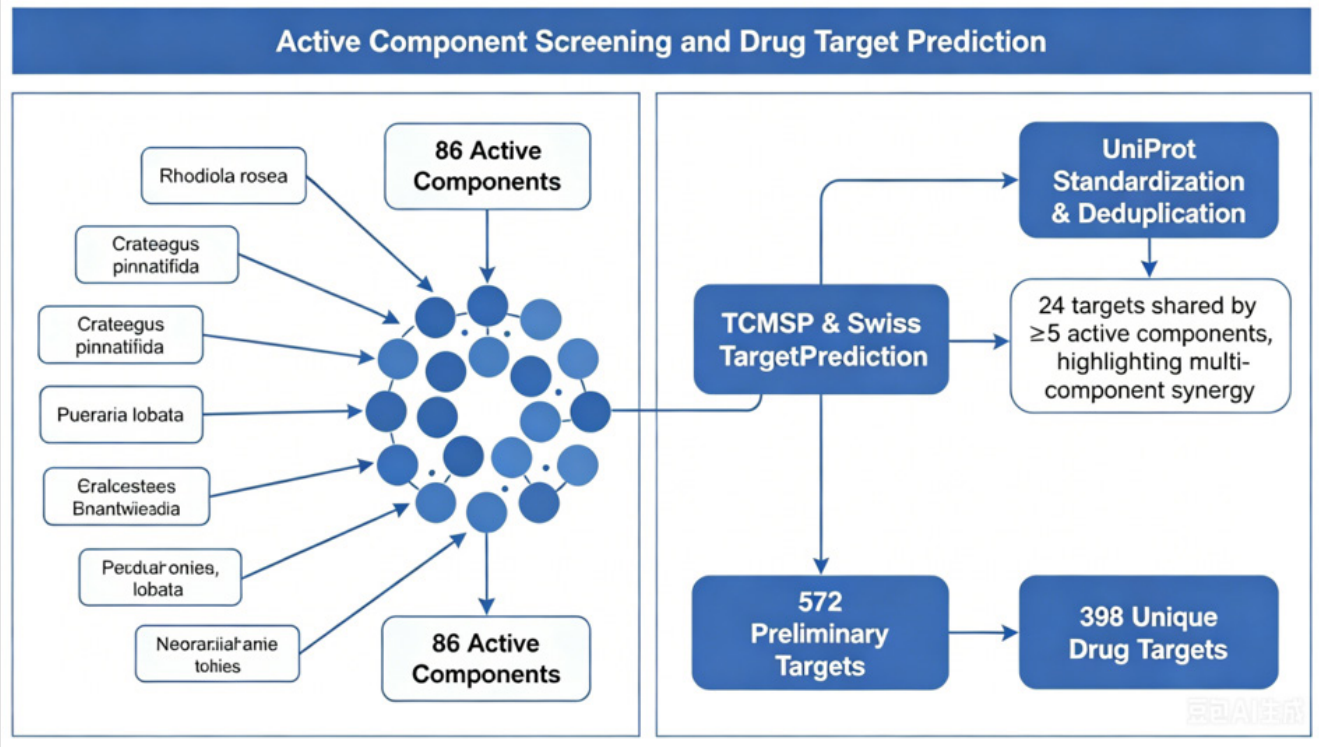

Figure 6.

Discussion

Molecular Interpretation of "Invigorating Qi and Activating Blood"

The NXT formula reflects the TCM principle of "invigorating Qi and activating blood." Astragalus, the Qi invigorating principal herb, regulates PI3K Akt and MAPK pathways to improve energy metabolism. Salidroside reduces inflammation via JAK2/STAT3 and NF κB; hawthorn flavonoids activate HIF 1 to reduce myocardial ischemia reperfusion injury; puerarin alleviates inflammation through TLR4 MyD88 NF κB; red yeast rice exerts lipid lowering effects via mTORC1 SREBPs; nattokinase regulates coagulation and fibrinolysis. Thus, "invigorating Qi and activating blood" at the molecular level represents an integration of metabolic support, inflammation inhibition, vasodilation, and thrombolysis.

Hub Roles of PI3K Akt and MAPK Signaling Pathways

PI3K Akt (18 targets, FDR=3.45×10^{-9}) and MAPK (10 targets) pathways are central. PI3K Akt is a major cell survival pathway that counteracts oxidative stress, apoptosis, and promotes angiogenesis. Many NXT components (salidroside, hawthorn flavonoids, puerarin, astragaloside IV) are predicted to activate this pathway. The crosstalk between PI3K Akt and MAPK further amplifies the multi pathway synergy.

Synergistic Regulation of Inflammation and Oxidative Stress

Enrichment of TNF, NF κB, and TLR pathways, together with Nrf2 mediated oxidative stress pathway, indicates that NXT simultaneously suppresses pro inflammatory cytokines (TNF, IL6) and activates endogenous antioxidant defenses (Nrf2/HO 1). Curcumin, rutin, and astaxanthin are key contributors. The GO terms "regulation of inflammatory response", "response to oxidative stress", and "negative regulation of apoptosis" are closely interconnected, aligning with the TCM concept of "phlegm stasis interlocking and toxin damaging the heart vessels."

Synergistic Mechanisms of Multi Module Components and the Four Dimensional Regulatory Network

The four functional modules (vasodilation, anti inflammation/antioxidation, metabolic support, lipid lowering/thrombolysis) do not act independently. For example, AKT1 is targeted by the vasodilation module (salidroside, hawthorn flavonoids) and the metabolic support module (astragaloside IV), creating a "multi component → single target" synergistic mode. TNF is targeted by multiple modules simultaneously. Molecular docking confirmed good binding affinities, supporting the predicted interactions.

Comparison with Previous Network Pharmacology Studies on Naoxintong

Our core targets (AKT1, TP53, TNF, MAPK1, STAT3) are consistent with previous studies. However, due to the inclusion of red yeast rice and nattokinase in the updated formula, our analysis revealed significant enrichment of the mTORC1 SREBPs pathway and arachidonic acid metabolism, which were less prominent in traditional NXT studies. Additionally, strong antioxidants (astaxanthin, rutin) elevated the Nrf2 ARE and Sirtuin1/PGC 1α pathways. Thus, the updated formula has a broader pharmacological spectrum.

Limitations

This study has several limitations:

(1) Database coverage may miss some hydrophilic components or metabolites;

(2) Target predictions require experimental validation (Western blot, RT qPCR, immunohistochemistry);

(3) Pharmacokinetic interactions among components were not modeled;

(4) The risk benefit of combining red yeast rice (natural statin) and nattokinase with prescription anticoagulants needs clinical evaluation.

Conclusion

This network pharmacology study systematically analyzed the updated Naoxintong formula. We identified 86 active components, 398 drug targets, and 143 therapeutic targets. PPI analysis revealed core targets including AKT1, TP53, TNF, IL6, STAT3, MAPK1, VEGFA, and EGFR. GO and KEGG analyses indicated that NXT acts through PI3K Akt, MAPK, TNF, AGE RAGE, HIF 1, NF κB, Nrf2, arachidonic acid metabolism, and mTORC1 SREBPs pathways. The formula can be divided into four functional modules that synergistically achieve vasodilation, anti inflammation/antioxidation, metabolic support, and lipid lowering/thrombolysis. Molecular docking validated the binding affinity between core components and targets. This study provides a theoretical basis for the precise clinical application and quality marker screening of the updated NXT formula and offers a methodological reference for studying the "four dimensional synergy" of TCM formulas.

References

1. Ru JL, Li P, Wang JN, Wei Zhou, Bohui Li, et al. (2014) TCMSP: a database of systems pharmacology for drug discovery from herbal medicines. J Cheminform 6: 13.
2. Daina A, Michielin O, Zoete V (2019) SwissTargetPrediction: updated data and new features for efficient prediction of protein targets of small molecules. Nucleic Acids Res 47(W1): W357-W364.
3. Daina A, Michielin O, Zoete V (2017) SwissADME: a free web tool to evaluate pharmacokinetics, drug likeness and medicinal chemistry friendliness of small molecules. Sci Rep 7: 42717.
4. Stelzer G, Rosen N, Plaschkes I, Shahar Zimmerman, Michal Twik, et al. (2016) The GeneCards Suite: from gene data mining to disease genome sequence analyses. Curr Protoc Bioinformatics 54: 1.30.1-1.30.33.
5. Hamosh A, Scott AF, Amberger JS, Carol A Bocchini, Victor A McKusick (2005) Online Mendelian Inheritance in Man (OMIM), a knowledgebase of human genes and genetic disorders. Nucleic Acids Res 33(suppl_1): D514-D517.
6. Piñero J, Ramírez Anguita JM, Saüch Pitarch J, Francesco Ronzano, Emilio Centeno, et al. (2020) The DisGeNET knowledge platform for disease genomics: 2019 update. Nucleic Acids Res 48(D1): D845-D855.
7. Szklarczyk D, Kirsch R, Koutrouli M, Katerina Nastou, Farrokh Mehryary, et al. (2023) The STRING database in 2023: protein protein association networks and functional enrichment analyses for any sequenced genome of interest. Nucleic Acids Res 51(D1): D638-D646.
8. Shannon P, Markiel A, Ozier O, Nitin S Baliga, Jonathan T Wang, et al. (2003) Cytoscape: a software environment for integrated models of biomolecular interaction networks. Genome Res 13(11): 2498-2504.
9. Tang Y, Li M, Wang J, Yi Pan, Fang Xiang Wu (2015) CytoNCA: a Cytoscape plugin for centrality analysis and evaluation of protein interaction networks. Biosystems 127: 67-72.
10. Sherman BT, Hao M, Qiu J, Xiaoli Jiao, Michael W Baseler, et al. (2022) DAVID: a web server for functional enrichment analysis and functional annotation of gene lists (2021 update). Nucleic Acids Res 50(W1): W216-W221.
11. Eberhardt J, Santos Martins D, Tillack AF, Stefano Forli (2021) AutoDock Vina 1.2.0: new docking methods, expanded force field, and Python bindings. J Chem Inf Model 61(8): 3891-3898.
12. Shang JF, Wen YL, Zhang XL, Guijinfeng Huang, Wenbin Chen, et al. (2025) Naoxintong capsule accelerates mitophagy in cerebral ischemia reperfusion injury via TP53/PINK1/PRKN pathway based on network pharmacology analysis and experimental validation. J Ethnopharmacol 336: 118721.
13. Xiu C, Luo H, Huang W, et al. (2025) Naoxintong is involved in the coagulation regulation of warfarin through the MAPK pathway. Drug Des Devel Ther 19: 4689-4715.
14. Chen X, Hu L, Wang R, Luo M, Wei C, et al. (2024) Uncovering the mechanism of Naoxintong capsule against hypertension based on network analysis and *in vitro* experiments. Chem Biol Drug Des 104(1): e14440.
15. Du K, Chen S, Wen J, Yang Liu, Suyi Liu, et al. (2025) Intelligence metabolic analysis combined with bioinformatics for investigating effect substance of Naoxintong capsule in treating carotid artery thrombosis. J Chromatogr A 1757: 466120.
16. Zhang H, Zhuang X, Li Z, Wang X (2024) Investigating the multitarget pharmacological mechanism of Rhodiola wallichiana var. cholaensis acting on angina pectoris using combined network pharmacology and molecular docking. J Thorac Dis 16(5): 3120-3135.
17. Kanehisa M, Furumichi M, Sato Y, Masayuki Kawashima, Mari Ishiguro Watanabe (2023) KEGG for taxonomy-based analysis of pathways and genomes. Nucleic Acids Res 51(D1): D587-D592.

ISSN: 2574-1241

DOI: 10.26717/BJSTR.2026.66.010289

Jiren Zhang . Biomed J Sci & Tech Res

Submission Link: https://biomedres.us/submit-manuscript.php